

1 **The implementation of NEMS GFS Aerosol Component**  
2 **(NGAC) Version 1.0 for global dust forecasting at**  
3 **NOAA/NCEP**

4  
5 **Cheng-Hsuan Lu<sup>1,2</sup>, Arlindo da Silva<sup>3</sup>, Jun Wang<sup>2</sup>, Shrinivas Moorthi<sup>4</sup>, Mian**  
6 **Chin<sup>3</sup>, Peter Colarco<sup>3</sup>, Youhua Tang<sup>5</sup>, Partha S. Bhattacharjee<sup>2</sup>, Shen-Po Chen<sup>1</sup>,**  
7 **Hui-Ya Chuang<sup>4</sup>, Hann-Ming Henry Juang<sup>4</sup>, Jeffery McQueen<sup>4</sup> and Mark Iredell<sup>4</sup>**

8 [1] {University at Albany, State University of New York, Albany, NY, USA}

9 [2] {I. M. Systems Group, Inc. at NOAA/NWS National Centers for Environmental  
10 Prediction, College Park, MD, USA}

11 [3] {NASA Goddard Space Flight Center, Greenbelt, MD, USA}

12 [4] {NOAA/NWS National Centers for Environmental Prediction, College Park, MD, USA}

13 [5] {NOAA/OAR Air Resources Laboratory, College Park, MD, USA}

14 Correspondence to: Cheng-Hsuan Lu (clu4@albany.edu)

15

16 **Abstract**

17 The NOAA National Centers for Environmental Prediction (NCEP) implemented NEMS GFS  
18 Aerosol Component (NGAC) for global dust forecasting in collaboration with NASA  
19 Goddard Space Flight Center (GSFC). NGAC Version 1.0 has been providing 5 day dust  
20 forecasts at 1°x1° resolution on a global scale, once per day at 00:00 Coordinated Universal  
21 Time (UTC), since September 2012. This is the first global system capable of interactive  
22 atmosphere aerosol forecasting at NCEP. The implementation of NGAC V1.0 reflects an  
23 effective and efficient transitioning of NASA research advances to NCEP operations, paving  
24 the way for NCEP to provide global aerosol products serving a wide range of stakeholders as  
25 well as to allow the effects of aerosols on weather forecasts and climate prediction to be  
26 considered.

# 1   **1   Introduction**

2   Aerosols affect the energy balance of Earth's atmosphere through the absorption and  
3   scattering of solar and thermal radiation (Mitchell, 1971). Aerosols also affect Earth's  
4   climate through their effects on cloud microphysics, reflectance, and precipitation (Twomey,  
5   1974; Albrecht, 1989; Jones et al., 1994; Lohmann et al., 2000). In addition to modulating  
6   Earth's climate and hydrological cycle (Ramanathan et al., 2001), aerosols are important for  
7   atmospheric chemistry, the biosphere, and public health. Aerosols can be viewed in their role  
8   as air pollutants because of their adverse health effects (Pöschl, 2005). Long range transport  
9   of aerosols can affect the air quality and visibility far from the source regions (Prospero,  
10   1999; Jaffe et al., 2003; Colarco et al., 2004). In addition, aerosols may play a significant role  
11   in atmospheric oxidation processes (Andreae and Crutzen, 1997; Dickerson et al., 1997).  
12   Large amounts of mineral dust are deposited to the oceans (Duce et al., 1991; Prospero et al.,  
13   1996) and the atmospheric input is found to be important for marine productivity (Chen et al.,  
14   2007).

15   While the importance of aerosols on climate has long been established, it is only recently that  
16   the aerosol effects are being increasingly recognized as important for weather predictions  
17   (Perez et al., 2006; Mulcahy et al., 2014). Haywood et al. (2005) shows that the neglect of the  
18   radiative effects of mineral dust leads to systematic biases in the top-of-the-atmosphere  
19   radiative budget in the UK Met Office (UKMO) numerical weather prediction (NWP) model.  
20   By prescribing updated aerosol climatology in the European Centre for Medium-Range  
21   Weather Forecasts (ECMWF) NWP model, a shift in the African Easterly Jet (AEJ) in better  
22   agreement with observations is demonstrated in Tompkins et al. (2005) and improvements in  
23   local medium-range forecast skills and global seasonal-mean are shown in Rodwell and Jung  
24   (2008). A number of studies have suggested that aerosols can significantly impact severe  
25   weather, such as intensifying Pacific storm track (Zhang et al., 2007; Wang et al., 2014),  
26   modifying hurricane and tropical cyclones (Rosenfeld et al., 2012; Herbener et al., 2014),  
27   affecting deep convective storms and tornado intensity in the U.S. (Wang et al., 2009; Saide  
28   et al., 2015), and enhancing catastrophic floods in Southwest China (Fan et al., 2015).

29   Despite recent progress in atmospheric aerosol modeling, the physical processes crucial for  
30   modeling aerosol effects are either poorly represented or outright missing in National Centers  
31   for Environmental Prediction (NCEP) global models. The NCEP's Global Forecast System  
32   (GFS) is the cornerstone of NCEP's operational production suite of numerical guidance. The

1 atmospheric forecast model used in the GFS is global spectrum model (GSM) with a  
2 comprehensive physics suite (see the GFS webpage at  
3 <http://www.emc.ncep.noaa.gov/GFS/doc.php>). Until now, the model only considers aerosol  
4 radiative effects and the aerosol distributions are prescribed based on a global climatological  
5 aerosol database (Hess et al., 1998).

6 Efforts to develop prognostic aerosol capability in NCEP global models have been underway  
7 in the last few years, which in turn is part of NCEP's modeling development efforts toward a  
8 unified modeling framework. Specifically, NCEP is developing NOAA Environmental  
9 Modeling System (NEMS) as its next-generation operational system (Black et al., 2007,  
10 2009) and has collaborated with NASA/Goddard Space Flight Center (GSFC) to develop  
11 NEMS GFS Aerosol Component (NGAC) for predicting the distribution of atmospheric  
12 aerosols (Lu et al., 2010; 2013). NGAC is the first on-line (interactive) atmospheric aerosol  
13 forecast system at NCEP. It consists of two key modeling components: (1) the GFS within  
14 the NEMS architecture (NEMS GFS) and (2) the on-line aerosol module based on Goddard  
15 Chemistry Aerosol Radiation and Transport (GOCART) model. The advantages for taking  
16 the so-called on-line approach include: (1) consistency: no spatial-temporal interpolation and  
17 the use of the same physics parameterization, (2) efficiency: lower overall CPU costs and  
18 easier data management, and (3) interaction: allows for aerosol feedback to meteorology.

19 NGAC Version 1.0 (NGAC V1.0) has been implemented and became operational at NCEP  
20 since September 2012. It provides real-time short-range (5 day) forecasts of dust aerosols  
21 with global coverage. The development of a global aerosol forecast system in turn provides a  
22 first step toward an aerosol data assimilation capability at NCEP. The rationale for  
23 developing the global aerosol forecasting and data assimilation capabilities at NCEP includes:  
24 (1) to improve weather forecasts and climate predictions by taking into account of aerosol  
25 effects on radiation and clouds, (2) to improve the handling of satellite observations by  
26 properly accounting for aerosol effects during the assimilation procedure; (3) to provide  
27 aerosol (lateral and upper) boundary conditions for regional air quality predictions; and (4) to  
28 provide global aerosol products to meet the stakeholder needs such as air quality, UV index,  
29 visibility, ocean productivity, solar energy production, and sea surface temperature (SST)  
30 retrievals.

31 Aerosol modeling, traditionally serving regional air quality and climate communities, has  
32 seen rapid development at several operational and research NWP centers in the last few years

1 (Reid et al., 2011; Benedetti et al., 2011, 2014). This includes NCEP (discussed in this  
2 paper), ECMWF (Benedetti et al., 2009; Morcrette et al., 2009), UKMO (Woodward 2001,  
3 2011), Naval Research Laboratory (NRL, Zhang et al., 2008; Westphal et al., 2009), NASA  
4 Global Modeling and Assimilation Office (GMAO, Colarco et al., 2010), Japan  
5 Meteorological Agency (JMA, Tanaka et al., 2003), and Barcelona Supercomputing Centre  
6 (BSC, Perez et al., 2011; Basart et al., 2012). In addition, the efforts to develop regional and  
7 global multi-model ensemble for aerosol prediction are underway (Sessions et al., 2015),  
8 offering aerosol products for research applications and eventually operational use. The  
9 implementation of NGAC V1.0 at NCEP not only contributes to the NCEP production suite  
10 but also to the international efforts for multi-model ensembles.

11 In this paper, we describe the development and implementation of NGAC V1.0 at NCEP. In  
12 Sect. 2, we describe the model configuration. In Sect. 3, we present the operational  
13 implementation of NGAC V1.0. In Sect. 4, we present the results of NGAC V1.0 forecasts  
14 and the comparisons to other global aerosol models and observations. In Sect. 5, we  
15 demonstrate two examples of NGAC V1.0 applications. Section 6 provides concluding  
16 remarks.

17

## 18 **2 Model configuration**

### 19 **2.1 Atmospheric model: NEMS GFS**

20 The efforts to develop a unified modeling framework to streamline the interaction of forecast,  
21 analysis, and post-processing systems within NCEP have been underway since late 2000  
22 (Black et al., 2007, 2009). Specifically, NCEP is developing NEMS  
23 (<http://www.emc.ncep.noaa.gov/index.php?branch=NEMS>) with a component-based  
24 architecture following the Earth System Modeling Framework (ESMF, see  
25 <http://www.earthsystemmodeling.org>). The ESMF is a community effort to promote the  
26 exchange and reusability of earth system modeling components and to facilitate faster  
27 knowledge transfer and technology adaptation. The ESMF collaboration involves many of  
28 the major climate, weather and data assimilation efforts in the United States, including  
29 NOAA/NCEP, NASA/GMAO, NRL, NOAA Geophysical Fluid Dynamics Laboratory  
30 (GFDL), and the National Center for Atmospheric Research (NCAR).

1 The development of NEMS aims to develop a common superstructure for NCEP production  
2 suite. Other motivations include: (1) to reduce overhead costs and provide a flexible  
3 infrastructure in the operational environment, (2) to modularize large pieces of the systems  
4 with ESMF components and interfaces, and (3) to enable NOAA contribution to the National  
5 Unified Operational Prediction Capability (NUOPC) with Navy and Air Force.

6 The NEMS is organized into collections of components with standardized interfaces, arranged  
7 in a hierarchical structure. Currently the GFS, the B-grid version of the Non-hydrostatic  
8 Multi-scale Model (NMM-B), and the Flow-following finite-volume Icosahedral Model  
9 (FIM) have been placed under the NEMS-atmosphere framework. A unified parallelized I/O  
10 package is developed to handle the synchronous production and writing of history files, which  
11 in turn has been linked with NCEP's unified post-processing system. The FIM atmosphere  
12 model is developed by NOAA Earth System Research Laboratory (ESRL) for global weather  
13 prediction research. The NMM-B model, developed by NCEP, is the forecast model for the  
14 North American Meso-scale Forecast System (NAM) providing operational meso-scale  
15 weather forecasts since October 2011. The NEMS version of GFS (referred to as NEMS GFS  
16 in this paper) consists of the same spectral dynamic core and physics parameterizations as the  
17 operational GFS with the following exceptions. First, GFS atmospheric model has been  
18 restructured to include separate components for the model's dynamics and physics as well as  
19 a coupler through which information is passed between the dynamics and physics. Despite  
20 extensive use of ESMF superstructure, infrastructure and utilities in NEMS, the underlying  
21 science code, however, remains the same as the operational GFS. Second, enhanced I/O and  
22 post-processing capabilities are introduced in the NEMS GFS. These include an option to  
23 output history files in native Gaussian grids instead of spectral grids and an option to run  
24 model integration in parallel to post-processing. Third, GFS physics parameterizations have  
25 been re-structured with a flexible interface, allowing it to be called by other dynamic cores.  
26 This option to assemble GFS physics as the NEMS unified physics package again reflects  
27 NCEP's modeling strategy toward a unified and yet flexible modeling infrastructure.

28 The NEMS has been under active development. Efforts to incorporate non-atmospheric  
29 components, e.g., ocean, wave, and sea ice models, are underway. The coupling  
30 infrastructure is based on the ESMF and NUOPC Layer code and conventions. Development  
31 is also made to enable emerging environmental prediction capabilities. The aerosol

1 forecasting capability, NGAC, discussed in this paper is virtually NEMS GFS with the  
2 prognostic aerosol option turned on.

### 3 **2.2 Aerosol model: GOCART**

4 Funded mainly by NASA Earth Science programs, the GOCART model was developed to  
5 simulate atmospheric aerosols (including sulfate, black carbon (BC), organic carbon (OC),  
6 dust, and sea-salt), and sulfur gases (Chin et al., 2000, 2002, 2003, 2004, 2007, 2009; Ginoux  
7 et al., 2001, 2004; Bian et al., 2010; Colarco et al., 2010; Kim et al., 2013). Originally  
8 GOCART was developed as an off-line Constituent Transport Model (CTM), driven by  
9 assimilated meteorological fields from the Goddard Earth Observing System Data  
10 Assimilation System (GEOS DAS, e.g., Chin et al., 2002). As part of the GEOS Version 4  
11 (GEOS-4) atmospheric model development at NASA GMAO, an ESMF compliant GOCART  
12 grid component has been developed (Colarco et al., 2010). When running within versions 4  
13 and 5 of GEOS (GEOS-4/5), the GOCART component provides aerosol processes such as  
14 emissions, sedimentation, dry and wet deposition (Fig. 1). Dynamic sources (wind-speed  
15 dependent) are considered for dimethyl sulfide (DMS), dust and sea salt. Emissions for SO<sub>2</sub>  
16 and carbonaceous aerosols arise from nature and anthropogenic sources, including biogenic,  
17 biofuel, anthropogenic, and biomass burning emissions. Aerosol chemistry currently uses  
18 prescribed OH, H<sub>2</sub>O<sub>2</sub>, and NO<sub>3</sub> fields for DMS and SO<sub>2</sub> oxidations. Aerosol sinks include  
19 wet removal (scavenging and rainout) and dry deposition (gravitational sedimentation and  
20 surface uptake). Advection, turbulent and convective transport is outside the scope of the  
21 GOCART component, being instead provided by the host atmospheric model. Unlike off-line  
22 CTM, this on-line aerosol module accurately utilizes winds, convective mass flux, and eddy  
23 diffusivity valid at each time step, without the need for temporal or spatial interpolation of  
24 any kind.

25 Research and development efforts have further enhanced GOCART modeling capabilities.  
26 The transition from off-line to on-line coupling approach mentioned above is an example. In  
27 addition, the GOCART grid component now has the option to ingest daily biomass burning  
28 emissions from the Quick Fire Emission Dataset (QFED, Darmenov and da Silva 2015).  
29 QFED emissions are based on fire radiative power retrievals from MODIS (Moderate  
30 Resolution Imaging Spectroradiometer, on board Aqua and Terra satellites). The inclusion of  
31 such observation-based, time-dependent emissions is important for the model to capture the  
32 large temporal-spatial variation of biomass burning emissions.

1 For dust, a topographic source function and mobilization scheme following Ginoux et al.  
2 (2001) is used. The dust emission parameterization depends on 10 m wind, the threshold  
3 velocity of wind erosion, and dust source function. The threshold velocity of wind erosion is  
4 determined from dust density, particle diameter, and surface soil wetness. The dust source  
5 function, representing the probability of dust uplifting, is determined from surface bareness  
6 and topographical depression features. Surface bareness is identified from the  $1^{\circ} \times 1^{\circ}$   
7 vegetation data set derived from the Advanced Very High Resolution Radiometer (AVHRR)  
8 data (DeFries and Townshend, 1994). The static dust source function has been regridded on  
9 the GFS native T126 Gaussian grid for NGAC V1.0 (shown in Fig. 2). The maxima of dust  
10 source function are collocated with the climatologically active dust sources or so-called dust  
11 hot spots. The most evident examples are the Sahara desert in north Africa, the Bodele  
12 depression over Chad, the Syrian desert in mid-East, the Taklimakan desert in northwest  
13 China, the Lake Eyre basin in Australia, the Sonoran desert in southwest California, the  
14 Namibian sources in southwest Africa, and Patagonian desert and Andean Plateau in the  
15 Andes.

### 16 **2.3 Coupling NEMS GFS with GOCART**

17 The GOCART grid component originally developed for GEOS-4/5 is fairly independent of  
18 the host atmospheric model, encapsulating the basic aerosol production and loss functionality.  
19 Consistent with standard ESMF architecture, the interfaces linking GOCART and NEMS  
20 GFS have been isolated into coupler components. Figure 3 shows the integration run stream  
21 of NGAC. Coupler components are built to transfer and transform the data between NEMS  
22 GFS and GOCART. The physics-to-chemistry coupler performs several tasks including: (i)  
23 the vertical flip for 3-dimensional fields, as GOCART is top-down while NEMS GFS is  
24 bottom-up, (ii) unit conversion as different units are used in NEMS GFS and GOCART for  
25 some fields such as precipitation rate, and (iii) the calculations for these fields needed by  
26 GOCART such as inferring relative humidity and air density from ambient temperature and  
27 moisture fields. After running GOCART, the chemistry-to-physics coupler transfers updated  
28 3-dimensional aerosol fields and 2-dimensional aerosol diagnosis fields from GOCART to  
29 NEMS GFS.

30 GOCART in GEOS-4/5 has been implemented in NEMS GFS 'as is' except for emission  
31 budget. As in GEOS-4/5 (Colarco et al., 2010), the spatial distribution and intensity of dust  
32 sources in NGAC V1 follows from Ginoux et al. (2001). Owing to differences in the GEOS-

1 4/5 meteorology and resolution relative to NEMS GFS, the global scaling constant for dust  
2 emissions (see equation (2) in Ginoux et al. (2001)) has been adjusted from  $C = 0.375 \mu\text{g s}^2$   
3  $\text{m}^{-5}$  as in GEOS-4/5 to  $C = 1 \mu\text{g s}^2 \text{m}^{-5}$  in NGAC. This adjustment is determined from  
4 sensitivity experiments, allowing NGAC V1 to obtain dust emission budget comparable to  
5 GEOS-4/5. Despite the ESMF flavor in how GOCART is implemented, GOCART is  
6 incorporated into NEMS GFS as a column process similar to how ozone physics was  
7 incorporated. It updates 3-dimensional aerosol loading after physical processes, ran at the  
8 same grid as physics and dynamics, and is fully coupled with physics and dynamics at each  
9 time step.

10

### 11 **3 NGAC V1.0 operational implementation**

12 A phased approach is used to manage the operational implementation of NGAC at NCEP.  
13 The first phase is to produce dust-only guidance, the second phase is to produce the full suite  
14 of aerosol forecasts (including dust, sea salt, sulfate, and carbonaceous aerosols), and the third  
15 phase is to produce aerosol analysis using NGAC forecasts as first guess. Only the initial  
16 deployment undertaken in 2012 is discussed in this paper.

17 Effective on 11 September 2012, starting with the 00:00 UTC cycle, NCEP has begun to run  
18 and disseminate data from the NGAC V1.0 system at T126 L64 resolution. It provides 5 day  
19 dust forecasts, once per day for the 00:00 UTC cycle. Information on accessing NGAC  
20 model output is provided in the Appendix. Daily web-based presentation of NGAC V1.0 dust  
21 forecasts is available at the EMC NGAC webpage:  
22 <http://www.emc.ncep.noaa.gov/gmb/NGAC/html/realtime.ngac.html>. The website displays  
23 aerosol optical depth (AOD) at 550 nm and surface mass concentrations over global domain  
24 and several regional domains (e.g., trans-Atlantic region, Asia, and Continental US (CONUS)  
25 regions).

26 Model configurations in NGAC V1.0 are same as those specified in operational high-  
27 resolution GFS runs with the following exceptions. First, NGAC uses Relaxed Arakawa-  
28 Schubert scheme (the RAS scheme, Moorthi and Suarez, 1992, 1999) while GFS uses  
29 Simplified Arakawa-Schubert scheme (the SAS scheme, Han and Pan, 2011). Enhanced  
30 tracer treatment (e.g., convective transport and tracer scavenging) has been incorporated into  
31 the RAS scheme, providing critical capability needed for aerosol modeling. Second, NGAC



1 V1.0 is run at coarser spatial resolution (T126 L64, ~ 110 km) than GFS. In February 2015,  
2 GFS was upgraded from Eulerian T574 (~ 27 km) to Semi-Lagrangian T1534 (~ 13 km).  
3 NGAC V1.0, however, remains Eulerian T126 as of October 2015. Third, NGAC V1.0  
4 produces history files and post-processed products concurrently while GFS produces post-  
5 processed products after history files being written out.

6 Dust initial conditions are taken from the 24 h NGAC V1.0 forecast from previous day while  
7 meteorological initial conditions are down-scaled from high-resolution Global Data  
8 Assimilation System (GDAS) analysis. Note the interaction of GOCART aerosol fields and  
9 GFS's radiation package has been disabled in NGAC V1.0. This configuration that aerosols  
10 are not radiatively coupled to AGCM is intended to facilitate aerosol modeling development  
11 in the near term. Once the prognostic aerosol capability reaches desired maturity level, this  
12 aerosol-radiation decoupled configuration will be changed allowing the aerosol direct and  
13 semidirect radiative effects to be accounted for.

#### 14 **4 NGAC results**

15 In this section, the results of operational NGAC V1.0 forecasts are presented. NCEP is  
16 currently working toward the phase-two NGAC implementation (Lu et al., 2016). The NGAC  
17 V2 includes full-suite of aerosols using near-real-time smoke emissions from satellite fire  
18 products. The NGAC upgrade will produce total AOD, allowing us to evaluate NGAC results  
19 beyond dust-dominated regions. Efforts are underway to evaluate experimental NGAC V2  
20 with other models (ICAP MME and GSFC's GEOS-5), in-situ observations at AERONET  
21 sites throughout the globe, and aerosol retrievals from multiple satellites, including MODIS,  
22 Visible Infrared Imaging Radiometer Suite (VIIRS) and Cloud-Aerosol Lidar with  
23 Orthogonal Polarization (CALIOP). In this paper, only concise model results are presented as  
24 the paper mainly provides the programmatic aspects of NGAC development and  
25 implementation.

#### 26 **4.1 Dust emissions and budget**

27 Figure 4 shows the annual dust emissions calculated from the first year NGAC V1.0  
28 production (the September 2012–September 2013 period). The similarity between the annual  
29 dust emissions and the dust source function (shown in Fig. 2) indicates that the source  
30 function is of central importance in determining dust uplifting relative to other parameters. In

1 the Ginoux et al. (2001) dust emission scheme, a global scaling factor ( $C$ , equal to  $1 \mu\text{g s}^2 \text{m}^{-5}$ )  
2  $^5$ ) is used to scale total dust flux to yield a total emission about 1800-2000  $\text{Tg yr}^{-1}$ . This factor  
3 is adjusted to  $0.375 \mu\text{g s}^2 \text{m}^{-5}$  in GEOS-4/5 owing to differences in the GEOS-4 meteorology  
4 relative to previous version of GEOS-DAS assimilated meteorology. As we adopted the on-  
5 line version of GOCART from GEOS-4/5 into NEMS GFS, the scaling factor is reverted back  
6 to  $1 \mu\text{g s}^2 \text{m}^{-5}$  to account for the differences in AGCM and resolution (i.e.,  $0.25^\circ$  resolution for  
7 GEOS-5 and  $\sim 1^\circ$  resolution for NEMS GFS).

8 Table 1 provides a summary of NGAC V1.0 calculated annual emission, burden, and lifetime  
9 (or atmospheric residence time) relative to other similar global aerosol models, including  
10 three versions of GOCART results and the models participating in the Aerosol Comparisons  
11 between Observations and Models (AeroCom) model intercomparison studies  
12 (<http://aerocom.met.no/aerocomhome.html>). The three GOCART results are from on-line  
13 GEOS4-GOCART (Colarco et al., 2010) and off-line GOCART CTM driven by two versions  
14 of GEOS DAS meteorological analyses (Chin et al., 2009; Ginoux et al., 2001).

15 Large difference (diversity) are found in emissions, burdens, and lifetimes within the  
16 AeroCom models, which is primarily related to the differences in the emission  
17 parameterizations, the particles sizes, the meteorological fields and model configuration used  
18 in the individual models (Textor et al., 2006). The simulated total dust emissions, annual  
19 burden, and lifetime in NGAC V1.0 are within the range of the AeroCom models. The annual  
20 emissions are similar in NGAC V1.0 and on-line GEOS4-GOCART ( $1980 \text{ Tg yr}^{-1}$  versus  
21  $1970 \text{ Tg yr}^{-1}$ ). In NGAC V1.0, the lifetime is about one and a half days shorter than in on-line  
22 GEOS4-GOCART (4.3 days versus 5.85 days) and the annual burden is about 30% lower  
23 ( $21.9 \text{ Tg}$  versus  $31.6 \text{ Tg}$ ). The results suggest more efficient removal processes in NGAC  
24 V1.0 than in GEOS4.

## 25 **4.2 Aerosol optical depth**

26 In this section we present the results of NGAC V1.0 dust distributions. We first compare  
27 NGAC dust AOD to dust AOD from GEOS-5 and total AOD from MODIS onboard Terra.  
28 Figure 5 shows monthly-mean dust distributions over the subtropical Atlantic region at  
29 different seasons. The source regions over the Sahara and Sahel are clearly shown as well as  
30 the patterns of long-range dust transport. Trade winds steer African dust westward across the  
31 Atlantic ocean, covering vast areas of the North Atlantic and sometime reaching the Americas

1 (e.g., the Caribbean, southeastern United States, Central America, and Amazon basin). This  
2 has implications for air quality, public health, climate, and biogeochemical cycle. For  
3 instance, about half of the annual dust supply to the Amazon basin is emitted from a single  
4 source in the Sahara, the Bodele depression (Koren et al., 2006).

5 While elevated dust off the western Africa coast is persistent through the seasons, the models  
6 and satellite observations show a clear latitudinal shift of the dust plume over the tropical  
7 Atlantic from winter to summer. This seasonal shift has been attributed to the movements of  
8 the Inter Tropical Convergence Zone (ITCZ) which occupies its southernmost location in  
9 winter and northernmost location in summer (Huser et al., 1997; Ginoux et al., 2001). The  
10 results are consistent with the seasonal cycle discussed in Knippertz and Todd (2012) in  
11 which detailed descriptions of meteorological processes controlling the emissions and  
12 transport of African dust are provided.

13 The comparison of model forecasts to L1.5 AERosol RObotic NETwork (AERONET) AOD at  
14 550 nm for 2013-2014 period at six stations is shown in Fig. 6. AERONET AOD at 550 nm  
15 is computed using logarithmic interpolation between AOD values at 440 nm and 675 nm. We  
16 bin the AERONET observations within one-hour time window centered at NGAC synoptic  
17 output times of 03:00, 06:00, 09:00, 12:00, 15:00, 18:00, 21:00, and 24:00 UTC. The  
18 calculation of monthly mean requires a minimum of 5 days with valid values. We show the  
19 comparison of the model AOD to AERONET observations, including the time series, a scatter  
20 plot, a fractional distribution histogram (PDF) of the model and observed AOD, and some  
21 statistics including mean biases, root-mean-square errors, linear fit parameters, and correlation  
22 coefficients. Among the six stations included in the comparison, three sites are located in  
23 dust-prone Sahara-Sahel region (Dakar, Ilorin, and Banizoumbou), one site is located in dust-  
24 prone Middle East area (Sede Boker), and two sites are located in tropical Atlantic Ocean  
25 region (Cape Verde and La Parguera). The Dakar site is located in Senegal, North Africa near  
26 the dust source region. The Ilorin site, located in Guinea Savanna zone, experiences dust and  
27 episodic smoke aerosols. The Banizoumbou site, located in the Sahel region, is influenced  
28 predominantly by dust transport from the Sahara. For the two ocean sites, Cape Verde is  
29 influenced by dust outflow from Saharan sources while La Parguera is influenced by long-  
30 range transport of Saharan dust. The Middle East site, Sede Boker, is located in the Negev  
31 desert of Israel and experiences mainly dust and urban aerosols. At these sites except for  
32 Ilorin, NGAC V1.0 simulations are found to capture the seasonal variability in the dust

1 loading. Overall, NGAC V1.0 shows similar seasonal variability to and is well correlated  
2 with the AERONET observations.

3

## 4 **5 NGAC applications**

5 NGAC V1.0 provides 2- and 3-dimensional aerosol products at  $1^{\circ}\times 1^{\circ}$  resolution on a global  
6 scale. Potential usage for these aerosol products includes, but is not limited to: AOD at 340  
7 nm for UV index forecasts; AOD at 550 nm for multi-model ensemble and aerosol data  
8 assimilation; AOD at 860 nm for AVHRR SST retrievals; AOD at  $11.1\ \mu\text{m}$  for the  
9 Atmospheric Infrared Sounder (AIRS) temperature retrievals; three dimensional dust mixing  
10 ratios for atmospheric correction; dust column mass density, emission and removal fluxes for  
11 aerosol budget study; dust deposition fluxes for ocean productivity and dust surface mass  
12 concentrations for air quality. Here we present two examples of NGAC product applications.

### 13 **5.1 Multi-model ensemble**

14 The International Cooperative for Aerosol Prediction (ICAP), consisting of forecasting center  
15 model developers and remote sensing data providers, began meeting in April 2010 to discuss  
16 issues relevant to the operational aerosol forecasting (Benedetti, 2011; Reid et al., 2011).  
17 ICAP members created a developmental global multiple-model ensemble (MME) to explore  
18 probabilistic aerosol prediction and assess relative differences among models (Sessions et al.,  
19 2015). Consensus ICAP forecasting began in early 2011 and the experimental ICAP-MME  
20 became quasi-operational for public release in 2015. Current ICAP MME products include  
21 total AOD ensemble from four complete aerosol forecast models from NRL, ECMWF, JMA,  
22 and GMAO and three dust-only models from NCEP, UKMO, and BSC. Figure 7 shows the  
23 dust AOD from ICAP-MME (with 7 members) and NGAC V1.0, valid at 12:00 UTC 4 July  
24 2015. Spatial pattern of dust loading from NGAC V1.0 is consistent with the ICAP-MME,  
25 with elevated dust AOD located in the Sahara, the Arabian Peninsula, and Asia as well as  
26 evident long range trans-Atlantic transport of Saharan dust reaching southeastern United  
27 States.

28 Dust forecasts from NGAC V1.0 also contributes to the regional multi-model ensemble  
29 produced by WMO Sand and Dust Storm Warning Advisory and Assessment System (SDS-  
30 WAS) Regional Center for Northern Africa, Middle East, and Europe, hosted at BSC, Spain  
31 (<http://sds-was.aemet.es>). Participation in ICAP-MME and WMO SDS-WAS multi-model

1 ensemble provides a continuous and independent assessment of the quality of NCEP global  
2 dust products. Overall, NGAC V1.0 forecasts are found to be comparable to that produced by  
3 other domestic and international modeling centers.

## 4 **5.2 Dynamic lateral boundary conditions for regional models**

5 An example on using NGAC dust information to improve regional air quality forecasts is  
6 presented here. Under a NOAA-EPA partnership, NOAA is undertaking the responsibility to  
7 develop and maintain the National Air Quality Forecasting (AQF) system (Davidson et al.  
8 2004). The AQF system is based on EPA Community Multi-scale Air Quality (CMAQ)  
9 model (Byun and Schere, 2006) driven by meteorological forecasts from NCEP North  
10 American Meso (NAM) Model (see the NAM webpage at  
11 <http://www.emc.ncep.noaa.gov/?branch=NAM>). Static lateral boundary conditions (LBCs)  
12 assuming no dust from outside the model boundary are currently used.

13 Two CMAQ runs are conducted for the July 2010 period. The baseline run uses static LBCs  
14 and the experimental run uses dynamic LBCs from NGAC V1.0. Figure 8 shows the  
15 observed and modeled surface Particulate Matter smaller than 2.5 micron (PM<sub>2.5</sub>) at two  
16 AIRNOW stations in the southeast region. Table 2 presents the statistic results of the CMAQ  
17 compared to the EPA AIRNOW PM<sub>2.5</sub>. It is found that the incorporation of dynamic LBCs  
18 from NGAC V1.0 reduces model biases and improves correlation. Clearly, the inclusion of  
19 long-range dust transport through dynamic LBCs leads to significant improvements in CMAQ  
20 forecasts during dust intrusion episodes.

21

## 22 **6 Conclusions**

23 NASA/GMAO's GOCART aerosol module has been implemented into NEMS GFS at NCEP  
24 through NOAA/NCEP-NASA/GSFC collaborations. While NGAC has the capability to  
25 forecast dust, sulfate, sea salt, and carbonaceous aerosols, the initial phase-one  
26 implementation is to establish dust-only numerical guidance. NGAC Version 1.0,  
27 implemented in September 2012, provides the first operational global dust forecasting  
28 capability at NOAA. Its AOD product has been incorporated into global and regional multi-  
29 model ensemble products (ICAP and WMO SDS-WAS, respectively) in quasi-operational  
30 mode.

1 The NGAC V1.0 dust forecasts are routinely verified using AOD observations from space-  
2 borne MODIS and ground-based AERONET. NGAC V1.0 results are also compared with  
3 those from other similar aerosol models. It is shown that the NGAC V1.0 simulated spatial  
4 distributions and seasonal variations are consistent with the observations. In addition, the  
5 emissions, burdens, and lifetime of dust aerosols in NGAC V1.0 are within the range of  
6 similar aerosol models.

7 While the initial NGAC implementation is limited in its scope (a dust-only system without  
8 aerosol data assimilation), it laid the ground work for various aerosol-related applications.  
9 Future operational benefits associated with the global aerosol forecasting system at NOAA  
10 includes:

- 11 – Enable operational global short-range multi-species aerosol prediction.
- 12 – Provide the first step toward an operational aerosol data assimilation capability at  
13 NCEP.
- 14 – Allow aerosol impacts on medium range weather forecasts to be considered.
- 15 – Provide global aerosol information for various applications, including satellite  
16 radiance data assimilation, satellite retrievals, SST analysis, and UV-Index forecasts.
- 17 – Allow NCEP to explore aerosol-cloud-climate interaction in the Climate Forecast  
18 System (CFS), as GFS is the atmosphere model of the CFS.
- 19 – Provide lateral aerosol boundary conditions for regional aerosol forecast system.

20

## 21 **Appendix: NGAC Output**

22 Output files and their contents for NGAC V1.0 (Q4FY12 Implementation)

23 (1) ngac.t00z.a2df\$HR, where HR=00, 03, ...,120:

24 2D products including

25 AER\_OPT\_DEP\_at550: dust aerosol optical depth at 550nm (dimensionless)

26 CR\_AER\_SFC\_MASS\_CON: coarse mode surface mass concentration ( $\text{kg m}^{-3}$ )

27 FN\_AER\_SFC\_MASS\_CON: fine mode surface mass concentration ( $\text{kg m}^{-3}$ )

28 CR\_AER\_COL\_MASS\_DEN: coarse mode column mass density ( $\text{kg m}^{-2}$ )

- 1 FN\_AER\_COL\_MASS\_DEN: fine mode column mass density ( $\text{kg m}^{-2}$ )
- 2 DUST\_EMISSION\_FLUX: dust emission fluxes ( $\text{kg m}^{-2} \text{sec}^{-1}$ )
- 3 DUST\_SEDIMENTATION\_FLUX: dust sedimentation fluxes ( $\text{kg m}^{-2} \text{sec}^{-1}$ )
- 4 DUST\_DRY\_DEPOSITION\_FLUX: dust dry deposition fluxes ( $\text{kg m}^{-2} \text{sec}^{-1}$ )
- 5 DUST\_WET\_DEPOSITION\_FLUX: dust wet deposition fluxes ( $\text{kg m}^{-2} \text{sec}^{-1}$ )
- 6
- 7 (2) ngac.t00z.a3df\$HR, where HR=00, 03, ..., 120:
- 8 3D products at model levels including
- 9 PRES: pressure (Pa)
- 10 RH: relative humidity (%)
- 11 TEMP: temperature (K)
- 12 DUST1: dust bin1 (0.1-1 micron) mixing ratio ( $\text{kg kg}^{-1}$ )
- 13 DUST2: dust bin2 (1-1.8 micron) mixing ratio ( $\text{kg kg}^{-1}$ )
- 14 DUST3: dust bin3 (1.8-3 micron) mixing ratio ( $\text{kg kg}^{-1}$ )
- 15 DUST4: dust bin4 (3-6 micron) mixing ratio ( $\text{kg kg}^{-1}$ )
- 16 DUST5: dust bin5 (6-10 micron) mixing ratio ( $\text{kg kg}^{-1}$ )
- 17
- 18 (3) ngac.t00z.aod\_\$NM, where NM=11p1um, 1p63um, 340nm, 440nm, 550nm, 660nm,
- 19 860nm:
- 20 Aerosol optical depth (dimensionless) at specified wavelengths (11.1, 1.63, 0.34, 0.44, 0.55,
- 21 0.66, and 0.86 micron)

## 22 **Data and code availability**

23 Products from the NCEP operational production suite are distributed and accessible to general  
24 users, free of charge, in real-time (typically no later than 3 hours after the data are created) at  
25 NOAA Operational Model Archive and Distribution System (NOMADS). Source code as  
26 well as relevant run scripts, parameters, and fixed field files can be obtained from NCEP  
27 Central Operations (NCO) ftp site at the following location:

1 <http://www.nco.ncep.noaa.gov/pmb/codes/nwprod/ngac.v1.0.0>

2 The NGAC V1.0 output is available in GRIB2 format on 1°x1°  
3 degree grid, with 3 hourly output out to 120 h. Users can access the NGAC V1.0 digital  
4 products from NOMADS at the following location:

5 <http://nomads.ncep.noaa.gov/pub/data/nccf/com/ngac>

6 NGAC V1.0 output instantaneous values of 3-dimensional dust mixing ratios for five particle  
7 sizes with effective radius at 1, 1.8, 3, 6, and 10 micron. The model also output time-  
8 averaged 2-dimensional diagnostics fields relevant to aerosol budget, such as emission fluxes.  
9 These aerosol fields are written out at GFS native Gaussian grid, and post-processed to  
10 GRIB2 format and regular 1°x1° degree grid. Dust AOD at 550 nm and other selected  
11 spectral is calculated from instantaneous dust distributions with aerosol optical properties  
12 based on Chin et al. (2002). NGAC V1.0 GRIB2 output files and their contents are listed in  
13 the Appendix.

14

## 15 **Acknowledgements**

16 The NGAC project has been supported by NASA Applied Science Program and NOAA-  
17 NASA-DOD Joint Center for Satellite Data Assimilation. The authors thank the principal  
18 investigators of the AERONET sites (Didier Tanre for Cape Verde, Dakar, and Banizoumbou,  
19 Rachel Pinker for Ilorin, Brent Holben for La Parguera, and Arnon Karnieli for Sede Boker)  
20 for the efforts in establishing and maintaining AERONET sites. Brent Holben leads the  
21 AERONET program and provided access to near-real-time L1.5 data set. The authors also  
22 appreciate the multi-model ensemble work done by the NRL (for ICAP) and BSC (for WMO  
23 SDS-WAS NA-ME-E Regional Center). The lead author C.-H. Lu is grateful for technical  
24 help and/or scientific input from her NCEP EMC colleagues, Wei-Yu Yang, Perry Shafran,  
25 Ho-Chun Huang, and Yuqiu Zhu. She also thanks her NCEP NCO colleagues for  
26 transitioning pre-operational NGAC V1.0 system into NCEP production, including Simon  
27 Hsiao, Xiaoxue Wang, Christine Caruso Magee, Jeff Ator, Boi Vuong, Rebecca Cosgrove and  
28 Daniel Starosta. The pre-implementation evaluation by Walter Sessions, Nick Nalli, Andy  
29 Harris, Craig Long, Gary Votaw, and Jeral Estupinan is also greatly appreciated.

30

31



## 1 **References**

- 2 Albrecht, B. A.: Aerosols, cloud microphysics and fractional cloudiness, *Science*, 245, 1227–  
3 1230, 1989.
- 4 Andreae, M. O. and Crutzen, P. J.: Atmospheric Aerosols: biogeochemical sources and role in  
5 atmospheric chemistry, *Science*, 276, 1052–1054, 1997.
- 6 Basart, S., Pérez, C., Nickovic, S., Cuevas, E., and Baldasano, J. M.: Development and  
7 evaluation of the BSC-DREAM8b dust regional model over Northern Africa, the  
8 Mediterranean and the Middle East, *Tellus B*, 64, 18539, doi:10.3402/tellusb.v64i0.18539,  
9 2012.
- 10 Benedetti, A., Morcrette, J.-J., Boucher, O., Dethof, A., Engelen, R. J., Fisher, M., Flentjes,  
11 H., Huneeus, N., Jones, L., Kaiser, J. W., Kinne, S., Mangold, A., Razinger, M., Simmons, A.  
12 J., Suttie, M., and the GEMS-AER team: Aerosol analysis and forecast in the European  
13 Centre for Medium-Range Weather Forecasts Integrated Forecast System: 2. Data  
14 assimilation, *J. Geophys. Res.*, 114, D13205, doi:10.1029/2008JD011115, 2009.
- 15 Benedetti, A., Reid, J. S., and Colarco, P. R.: International Cooperative for Aerosol Prediction  
16 (ICAP) Workshop On Aerosol Forecast Verification, *B. Am. Meteorol. Soc.*, 92, ES48–ES53,  
17 doi:10.1175/BAMS-D-11-00105.1, 2011.
- 18 Benedetti, A., Baldasano, J. M., Basart, S., Benincasa, F., Boucher, O., Brooks, M., Chen, J.-  
19 P., Colarco, P. R., Gong, S., Huneeus, N., Jones, L. T., Lu, S., Menut, L., Morcrette, J.-J.,  
20 Mulcahy, J., Nickovic, S., Perez Garcia-Pando, C., Reid, J. S., Sekiyama, T. T., Tanaka, T.  
21 Y., Terradellas, E., Westphal, D. L., Zhang, X.-Y., and Zhou, C.-H.: Operational dust  
22 forecasting, Chapter 10 in: *Mineral Dust: a Key Player in the Earth System*, edited by:  
23 Knippertz, P. and Stuut, J.-B., Springer Publications, Dodrecht, the Netherlands, ISBN 978-  
24 94-017-8977-6, 121–148, doi:10.1007/978-94-017-8978-3\_10, 2014.
- 25 Bian, H., Chin, M., Kawa, S. R., Yu, H., and Diehl, T.: Multi-scale carbon monoxide and  
26 aerosol correlations from MOPITT and MODIS satellite measurements and GOCART model:  
27 implication for their emissions and atmospheric evolutions, *J. Geophys. Res.*, 115, D07302,  
28 doi:10.1029/2009JD012781, 2010.
- 29 Black, T., Juang, H. M. H., Yang, W. Y., and Iredell, M.: An ESMF framework for NCEP  
30 operational models, in: *22nd Conference on Weather Analysis and Forecasting/18th*

1 Conference on Numerical Weather Prediction, Park City, UT, USA, 25–29 June 2007, Ameri.  
2 Met. Soc., J3.1, 2007.

3 Black, T., Juang, H. M. H., and Iredell, M.: The NOAA Environmental Modeling System at  
4 NCEP, Preprints, 23rd Conference on Weather Analysis and Forecasting/19th Conference on  
5 Numerical Weather Prediction, Omega, NE, USA, 1–5 June 2009, Ameri. Met. Soc., 2 A.6,  
6 2009.

7 Byun, D. W. and Schere, K. L.: Review of the governing equations, computational  
8 algorithms, and other components of the Models-3 Community Multiscale Air Quality  
9 (CMAQ) modeling system, *Appl. Mech. Rev.*, 59, 51-77, 2006.

10 Chen, Y., Mills, S., Street, J., Golan, D., Post, A., Jacobson, M., and Paytan, A.: Estimates of  
11 atmospheric dry deposition and associated input of nutrients to Gulf of Aqaba seawater, *J.*  
12 *Geophys. Res.*, 112, D04309, doi:10.1029/2006JD007858, 2007.

13 Chin, M., Savoie, D. L., Huebert, B. J., Bandy, A. R., Thornton, D. C., Bates, T. S., Quinn, P.  
14 K., Saltzman, E. S., and De Bruyn, W. J.: Atmospheric sulfur cycle in the global model  
15 GOCART: comparison with field observations and regional budgets, *J. Geophys. Res.*, 105,  
16 24689– 24712, 2000.

17 Chin, M., Ginoux, P., Kinne, S., Torres, O., Holben, B. N., Duncan, B. N., Martin, R. V.,  
18 Logan, J. A., Higurashi, A., and Nakajima, T.: Tropospheric aerosol optical thickness from  
19 the GOCART model and comparisons with satellite and sunphotometer measurements, *J.*  
20 *Atmos. Sci.*, 59, 461–483, 2002.

21 Chin, M., Ginoux, P., Lucchesi, R., Huebert, B., Weber, R., Anderson, T., Masonis, S.,  
22 Blomquist, B., Bandy, A., and Thornton, D.: A global aerosol model forecast for the  
23 ACEAsia field experiment, *J. Geophys. Res.*, 108, 8654, doi:10.1029/2003JD003642, 2003.

24 Chin, M., Chu, D. A., Levy, R., Remer, L. A., Kaufman, Y. J., Holben, B. N., Eck, T., and  
25 Ginoux, P.: Aerosol distribution in the Northern Hemisphere during ACE-Asia: results from  
26 global model, satellite observations, and sunphotometer measurements, *J. Geophys. Res.*, 109,  
27 D23S90, doi:10.1029/2004JD004829, 2004.

28 Chin, M., Diehl, T., Ginoux, P., and Malm, W.: Intercontinental transport of pollution and  
29 dust aerosols: implications for regional air quality, *Atmos. Chem. Phys.*, 7, 5501–5517,  
30 doi:10.5194/acp-7-5501-2007, 2007.

1 Chin, M., Diehl, T., Dubovik, O., Eck, T. F., Holben, B. N., Sinyuk, A., and Streets, D. G.:  
2 Light absorption by pollution, dust, and biomass burning aerosols: a global model study and  
3 evaluation with AERONET measurements, *Ann. Geophys.*, 27, 3439–3464,  
4 doi:10.5194/angeo-27-3439-2009, 2009.

5 Colarco, P., Schoeberl, M., Doddridge, B., Marufu, L., Torres, O., and Welton, E.: Transport  
6 of smoke from Canadian forest fires to the surface near Washington DC, *J. Geophys. Res.*,  
7 109, D06203, doi:10.1029/2003JD004248, 2004.

8 Colarco, P., da Silva, A., Chin, M., and Diehl, T.: Online simulations of global aerosol  
9 distributions in the NASA GEOS-4 model and comparisons to satellite and ground-based  
10 aerosol optical depth, *J. Geophys. Res.*, 115, D14207, doi:10.1029/2009JD012820, 2010.

11 Darmenov, A. and da Silva, A. M.: The Quick Fire Emissions Dataset (QFED) –  
12 Documentation of versions 2.1, 2.2 and 2.4, NASA Technical Report Series on Global  
13 Modeling and Data Assimilation, NASA/TM-2015–104606, Vol. 38, 211 pp., available at:  
14 <http://gmao.gsfc.nasa.gov/pubs/tm/>, last access: 18 December 2015.

15 Davidson, P. M., Seaman, N., Schere, K., Wayland, R. A., Hayes, J. L., and Carey, K. F.:  
16 National air quality forecasting capability: first steps toward implementation, in: Proceedings  
17 of Sixth Conf. on Atmos. Chem., Amer. Met. Soc., Seattle, WA, USA, 10–16 January 2004,  
18 J2.10, 2004.

19 DeFries, R. S., and Townshend, J. R. G.: NDVI-derived land cover classification at global  
20 scale, *Int. J. Remote Sensing*, 15, 3567–3586, 1994.

21 Dickerson, R. R., Kondragunta, S., Stenchikov, G., Civerolo, K. L., Doddridge, B. G., and  
22 Holben, B. N.: The impact of aerosols on solar ultraviolet radiation and photochemical smog,  
23 *Science*, 278, 827–830, 1997.

24 Duce, R. A.: The atmospheric input of trace species to the world ocean, *Global Biogeochem.*  
25 *Cy.*, 5, 193–259, 1991.

26 Fan, J., Rosenfeld, D., Yang, Y., Zhao, C., Leung, L. R., and Li, Z.: Substantial contribution  
27 of anthropogenic air pollution to catastrophic floods in Southwest China, *Geophys. Res. Lett.*,  
28 42, 6066–6075, doi:10.1002/2015GL064479, 2015.

1 Ginoux, P., Chin, M., Tegen, I., Prospero, J., Holben, B., Dubovik, O., and Lin, S.-J.: Sources  
2 and global distributions of dust aerosols simulated with the GOCART model, *J. Geophys.*  
3 *Res.*, 106, 20255–20273, 2001.

4 Ginoux, P., Prospero, J., Torres, O., and Chin, M.: Long-term simulation of dust distribution  
5 with the GOCART model: correlation with the North Atlantic Oscillation, *Environ. Modell.*  
6 *Softw.*, 19, 113–128, 2004.

7 Han, J. and Pan, H.-L.: Revision of convection and vertical diffusion schemes in the NCEP  
8 global forecast system, *Weather Forecast.*, 26, 520–533, 2011.

9 Haywood, J. M., Allan, R. P., Culverwell, I., Slingo, T., Milton, S., Edwards, J., and  
10 Clerbaux, N.: Can desert dust explain the outgoing longwave radiation anomaly over the  
11 Sahara during July 2003?, *J. Geophys. Res.*, 110, D05105, doi:10.1029/2004JD005232, 2005.

12 Herbener, S. R., van den Heever, S. C., Carrió, G. G., Saleeby, S. M., William, R., and  
13 Cotton, W. R.: Aerosol indirect effects on idealized tropical cyclone dynamics. *J. Atmos. Sci.*,  
14 71, 2040–2055, doi:10.1175/JAS-D-13-0202.1. 2014.

15 Hess, M., Koepke, P., and Schult, I.: Optical properties of aerosols and clouds: the software  
16 package OPAC, *B. Am. Meteorol. Soc.*, 79, 831–844, 1998.

17 Huneus, N., Schulz, M., Balkanski, Y., Griesfeller, J., Prospero, J., Kinne, S., Bauer, S.,  
18 Boucher, O., Chin, M., Dentener, F., Diehl, T., Easter, R., Fillmore, D., Ghan, S., Ginoux, P.,  
19 Grini, A., Horowitz, L., Koch, D., Krol, M. C., Landing, W., Liu, X., Mahowald, N., Miller,  
20 R., Morcrette, J.-J., Myhre, G., Penner, J., Perlwitz, J., Stier, P., Takemura, T., and Zender, C.  
21 S.: Global dust model intercomparison in AeroCom phase I, *Atmos. Chem. Phys.*, 11, 7781–  
22 7816, doi:10.5194/acp-11-7781-2011, 2011.

23 Husar, R., B., Prospero, J. M., and Stowe, L. L.: Characterization of tropospheric aerosols  
24 over the oceans with the NOAA advanced very high resolution radiometer optical thickness  
25 operational products, *J. Geophys. Res.*, 102, 16889–16909, 1997.

26 Jaffe, D., McKendry, I., Anderson, T., and Price, H.: Six “new” episodes of trans-Pacific  
27 transport of air pollutants, *Atmos. Environ.*, 37, 391–404, 2003.

28 Jones, D., Robarts, D. L., and Slingo, A.: A climate model study of indirect radiative forcing  
29 by anthropogenic sulphate aerosols, *Nature*, 370, 450–453, 1994.

1 Kim, D., Chin, M., Bian, H., Tan, Q., Brown, M. E., Zheng, T., You, R., Diehl, T., Ginoux,  
2 P., and Kucsera, T.: The effect of the dynamic surface bareness to dust source function,  
3 emission, and distribution, *J. Geophys. Res.*, 118, 1–16, doi:10.1029/2012JD017907, 2013.

4 Knippertz, P. and Todd, M. C.: Mineral dust aerosols over the Sahara: meteorological controls  
5 on emission and transport and implications for modeling, *Rev. Geophys.*, 50, RG1007,  
6 doi:10.1029/2011RG000362, 2012.

7 Koren, I., Kaufman, Y. J., Washington, R., Todd, M. C., Rudich, Y., Vanderlei Martins, J.,  
8 and Resenfeld, D.: The Bodele depressions: a single spot in the Sahara that provides most of  
9 the mineral dust to the Amazon forecast, *Environ. Res. Lett.*, 1, 014005, doi:10.1088/1748-  
10 9326/1/1/014005, 2006.

11 Lohmann, U., Feichter, J., Penner, J., and Leaitch, R.: Indirect effect of sulfate and  
12 carbonaceous aerosols: a mechanistic treatment, *J. Geophys. Res.*, 105, 12193–12206, 2000.

13 Lu, S., Huang, H.-C., Hou, Y.-T., Tang, Y., McQueen, J., da Silva, A., Chin, M., Joseph, E.,  
14 and Stockwell, W.: Development of NCEP Global Aerosol Forecasting System: an overview  
15 and its application for improving weather and air quality forecasts, in: *NATO Science for  
16 Peace and Security Series: Air Pollution Modelling and Its Application XX*, Springer  
17 Publications, Dordrecht, the Netherlands, ISBN 978-90-481-3810-4, 451–454,  
18 doi:10.1007/978-90-481-3812-8, 2010.

19 Lu, S., da Silva, A., Chin, M., Wang, J., Moorthi, S., Juang, H., Chuang, H.-Y., Tang, Y.,  
20 Jones, L., Iredell, M., and McQueen, J.: The NEMS GFS Aerosol Component: NCEP's  
21 Global Aerosol Forecast System, NCEP Office Note 472, Washington DC, USA, 26 pp.,  
22 available at: [http://www.lib.ncep.noaa.gov/ncepo\\_cenotes/2010s/](http://www.lib.ncep.noaa.gov/ncepo_cenotes/2010s/) (last access: 18 December  
23 2015), 2013.

24 Lu, S., Wang, J., Bhattacharjee, P., Zhang, X., Kondragunta, S., da Silva, A., McQueen, J.,  
25 Moorthi, S., Hou, Y., and Tallapragada, V.: The implementation of NEMS GFS Aerosol  
26 Component (NGAC) version 2: Global aerosol forecasting at NCEP using satellite-based  
27 smoke emissions, 5-8, *Joint Center for Satellite Data Assimilation Quarterly*, 53, available at:  
28 <http://www.jcsda.noaa.gov/news.php> (last access: 24 April 2016), doi:10.7289/V50C4SS7,  
29 2016.

30 Mitchell Jr., J.: The effect of atmospheric aerosols on climate with special references to  
31 temperature near the earth's surface, *J. Appl. Meteorol.*, 10, 703–714, 1971.

1 Moorthi, S. and Suarez, M. J.: Relaxed Arakawa–Schubert: a parameterization of moist  
2 convection for general circulation models, *Mon. Weather Rev.*, 120, 978–1002, 1992.

3 Moorthi, S. and Suarez, M. J.: Documentation of Version 2 of Relaxed Arakawa–Schubert  
4 Cumulus Parameterization With Moist Downdrafts, NOAA Technical report NWS/NCEP 99-  
5 01, NOAA/NCEP, College Park, MD, USA, 44 pp., 1999.

6 Morcrette, J.-J., Boucher, O., Jones, L., Salmond, D., Bechtold, P., Beljaars, A., Benedetti, A.,  
7 Bonet, A., Kaiser, J. W., Razinger, M., Schulz, M., Serrar, S., Simmons, A. J., Sofiev, M.,  
8 Suttie, M., Tompkins, A. M., and Untch, A.: Aerosol analysis and forecast in the European  
9 Centre for Medium-Range Weather Forecasts Integrated Forecast System: forward modeling,  
10 *J. Geophys. Res.*, 114, D06206, doi:10.1029/2008JD011235, 2009.

11 Mulcahy, J. P., Walters, D. N., Bellouin, N., and Milton, S. F.: Impacts of increasing the  
12 aerosol complexity in the Met Office global numerical weather prediction model, *Atmos.*  
13 *Chem. Phys.*, 14, 4749–4778, doi:10.5194/acp-14-4749-2014, 2014.

14 Pérez, C., Nickovic, S., Pejanovic, G., Baldasano, J. M., and Ozsoy, E.: Interactive dust  
15 radiation modeling: a step to improve weather forecasts, *J. Geophys. Res.*, 11, D16206,  
16 doi:10.1029/2005JD006717, 2006.

17 Pérez, C., Haustein, K., Janjic, Z., Jorba, O., Huneus, N., Baldasano, J. M., Black, T., Basart,  
18 S., Nickovic, S., Miller, R. L., Perlwitz, J. P., Schulz, M., and Thomson, M.: Atmospheric  
19 dust modeling from meso to global scales with the online NMMB/BSC-Dust model– Part 1:  
20 Model description, annual simulations and evaluation, *Atmos. Chem. Phys.*, 11, 13001–13027,  
21 doi:10.5194/acp-11-13001-2011, 2011.

22 Pöschl, U.: Atmospheric aerosols: composition, transformation, climate, and health effects,  
23 *Angew. Chem. Int. Edit.*, 44, 7520–7540, doi:10.1002/anie.200501122, 2005.

24 Prospero, J.: Long-term measurements of the transport of African mineral dust to the  
25 southeastern United States: implications for regional air quality, *J. Geophys. Res.*, 104,  
26 15917–15927, 1999.

27 Prospero, J. M., Barrett, K., Church, T., Dentener, F., Duce, R. A., Galloway, J. N., Levy II,  
28 H., Moody, J., and Quinn, P.: Atmospheric deposition of nutrients to the North Atlantic basin,  
29 *Biogeochemistry*, 35, 27–73, 1996.

1 Ramanathan, V., Crutzen, P. J., Kiehl, J. T., and Rosenfeld, D.: Aerosol, climate, and the  
2 hydrological cycle, *Science*, 294, 2119–2124, 2001.

3 Reid, J. S., Benedetti, A., Colarco, P. R., and Hansen, J. A.: International Operational Aerosol  
4 Observability Workshop, *B. Am. Meteorol. Soc.*, 92, ES21–ES24,  
5 doi:10.1175/2010BAMS3183.1, 2011.

6 Rodwell, M. J. and Jung, T.: Understanding the local and global impacts of model physics  
7 changes: an aerosol example, *Q. J. Roy. Meteor. Soc.*, 134, 1479–1497, doi:10.1002/qj.298,  
8 2008.

9 Rosenfeld, D., Woodley, W. L., Khain, A., Cotton, W. R., Carrió, G., Ginis, I., and Golden, J.  
10 H.: Aerosol effects on microstructure and intensity of tropical cyclones, *B. Am. Meteorol.*  
11 *Soc.*, 93, 987–1001, 2012.

12 Saide, P. E., Spak, S. N., Pierce, R. B., Otkin, J. A., Schaack, T. K., Heidinger, A. K., da  
13 Silva, A. M., Kacenelenbogen, M., Redemann, J., and Carmichael, G. R.: Central American  
14 biomass burning smoke can increase tornado severity in the U.S., *Geophys. Res. Lett.*, 42,  
15 956–965, doi:10.1002/2014GL062826, 2015.

16 Sessions, W. R., Reid, J. S., Benedetti, A., Colarco, P. R., da Silva, A., Lu, S., Sekiyama, T.,  
17 Tanaka, T. Y., Baldasano, J. M., Basart, S., Brooks, M. E., Eck, T. F., Iredell, M., Hansen, J.  
18 A., Jorba, O. C., Juang, H.-M. H., Lynch, P., Morcrette, J.-J., Moorthi, S., Mulcahy, J.,  
19 Pradhan, Y., Razinger, M., Sampson, C. B., Wang, J., and Westphal, D. L.: Development  
20 towards a global operational aerosol consensus: basic climatological characteristics of the  
21 International Cooperative for Aerosol Prediction Multi-Model Ensemble (ICAP-MME),  
22 *Atmos. Chem. Phys.*, 15, 335–362, doi:10.5194/acp-15-335-2015, 2015.

23 Tanaka, T. Y., Orito, K., Sekiyama, T. T., Shibata, K., Chiba, M., and Tanaka, H.:  
24 MASINGAR, a global tropospheric aerosol chemical transport model coupled with  
25 MRI/JMA98 GCM: model description, *Pap. Meteorol. Geophys.*, 53, 119–138, 2003.

26 Textor, C., Schulz, M., Guibert, S., Kinne, S., Balkanski, Y., Bauer, S., Berntsen, T., Berglen,  
27 T., Boucher, O., Chin, M., Dentener, F., Diehl, T., Easter, R., Feichter, H., Fillmore, D.,  
28 Ghan, S., Ginoux, P., Gong, S., Grini, A., Hendricks, J., Horowitz, L., Huang, P., Isaksen, I.,  
29 Iversen, I., Kloster, S., Koch, D., Kirkevåg, A., Kristjansson, J. E., Krol, M., Lauer, A.,  
30 Lamarque, J. F., Liu, X., Montanaro, V., Myhre, G., Penner, J., Pitari, G., Reddy, S., Seland,  
31 Ø., Stier, P., Takemura, T., and Tie, X.: Analysis and quantification of the diversities of

1 aerosol life cycles within AeroCom, *Atmos. Chem. Phys.*, 6, 1777–1813, doi:10.5194/acp-6-  
2 1777-2006, 2006.

3 Tompkins, A. M., Cardinali, C., Morcrette, J. J., and Rodwell, M.: Influence of aerosol  
4 climatology on forecasts of the African Easterly Jet, *Geophys. Res. Lett.*, 32, L10801,  
5 doi:10.1029/2004GL022189, 2005.

6 Twomey, S.: Pollution and the planetary albedo, *Atmos. Environ.*, 8, 1251–1256, 1974.

7 Wang, J., van den Heever, S. C., and Reid, J. S.: Central American biomass burning aerosols  
8 and severe weather over the south central United States, *Environ. Res. Lett.*, 4, 015003,  
9 doi:10.1088/1748-9326/4/1/015003, 2009.

10 Wang, Y., Wang, M., Zhang, R., Ghan, S., Lin, Y., Hu, J., Pan, B., Levy, M., Jiang, J., and  
11 Molina, M.: Assessing the effects of anthropogenic aerosols on Pacific storm track using a  
12 multiscale global climate model, *P. Natl. Acad. Sci. USA*, 111, 6894–6899,  
13 doi:10.1073/pnas.1403364111, 2014.

14 Westphal, D. L., Curtis, C. A., Liu, M., and Walker, A. L.: Operational aerosol and dust storm  
15 forecasting, in: WMO/GEO Expert Meeting on an International Sand and Dust Storm  
16 Warning System, IOP Conf. Series: Earth and Environ. Science, 7–9 November 2007,  
17 Barcelona Supercomputing Center (BSC), Barcelona, Spain, 7, doi:10.1088/1755-  
18 1307/7/1/012007, 2009.

19 Woodward, S.: Modeling the atmospheric life cycle and radiative impact of mineral dust in  
20 the Hadley Centre climate model, *J. Geophys. Res.*, 106, 18155–18166,  
21 doi:10.1029/2000JD900795, 2001.

22 Woodward, S.: Mineral Dust in HadGEM2, Tech. Note 87, Hadley Cent., Met Office, Exeter,  
23 UK, 2011.

24 Zhang, J., Reid, J. S., Westphal, D. L., Baker, N., and Hyer, E. J.: A system for operational  
25 aerosol optical depth data assimilation over global oceans, *J. Geophys. Res.*, 113, D10208,  
26 doi:10.1029/2007JD009065, 2008.

27 Zhang, R., Li, G., Fan, J., Wu, D. L., and Molina, M.: Intensification of Pacific storm track  
28 linked to Asian pollution, *P. Natl. Acad. Sci. USA*, 104, 5295–5299,  
29 doi:10.1073/pnas.0700618104, 2007.

30



1  
2  
3  
4

Table 1. Global annual emissions, annual burden and lifetime for dust aerosols<sup>a</sup>.

	Emissions (Tg yr <sup>-1</sup> )	Burden (Tg)	Lifetime (day)
NGAC V1.0	1980	21.9	4.3
On-line GEOS4	1970	31.6	5.85
Off-line GEOS4	3242	38.4	4.33
Off-line GEOS	1604-1956	31-40	6.6-7.3
AeroCom	1123 [514 – 4313]	15.8 [6.8 – 29.5 ]	4.6 [1.6 – 7.1]

5  
6  
7  
8  
9  
10  
11  
12  
13  
14

<sup>a</sup>Note: the top number is the NGAC V1.0 results from September 2012–September 2013, the second number is the results of on-line GEOS4-GOCART simulations (Table 1 in Colarco et al., 2010), the third number is the results of off-line GEOS4-GOCART model (Table 1 in Colarco et al., 2010 which in turn is provided by Mian Chin using the off-line GEOS4-GOCART model described in Chin et al., 2009), the fourth number is the results of off-line GEOS-GOCART model (Table 2 in Ginoux et al., 2001), and the fifth number is the average of the AeroCom models with the range of the models in parentheses (Table 3 in Huneus et al., 2011).

1 Table 2. Statistic results comparing CMAQ model results with EPA AIRNOW PM2.5.  
 2 The mean bias (MB) and correlation (R) are calculated for the baseline run using static  
 3 LBCs and the experimental run using NGAC LBCs.

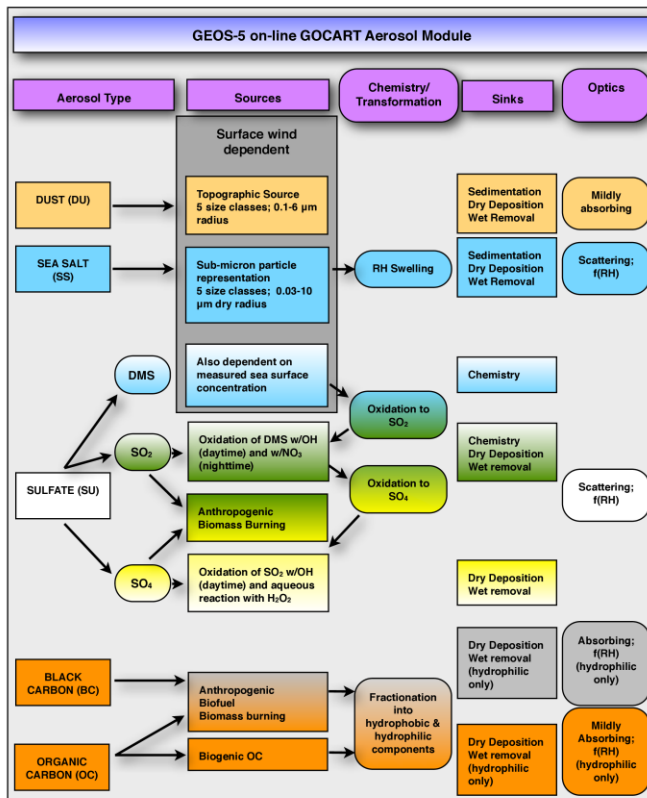
Domain/Period	CMAQ Baseline	CMAQ Experimental
Whole domain, July 1 - Aug 3	1 1 MB = -2.82, R = 0.42	MB = -0.88, R = 0.44
South of 38°N, East of 105°W July 1- Aug 3	MB = -4.54, R=0.37	MB = -1.76, R = 0.41
Whole domain, July 18 – July 30	MB = -2.79, R = 0.31	MB = -0.33, R = 0.37
South of 38°N, East of 105°W July 18 – July 30	MB = 4.79, R=0.27	MB = -0.46, R = 0.41

4

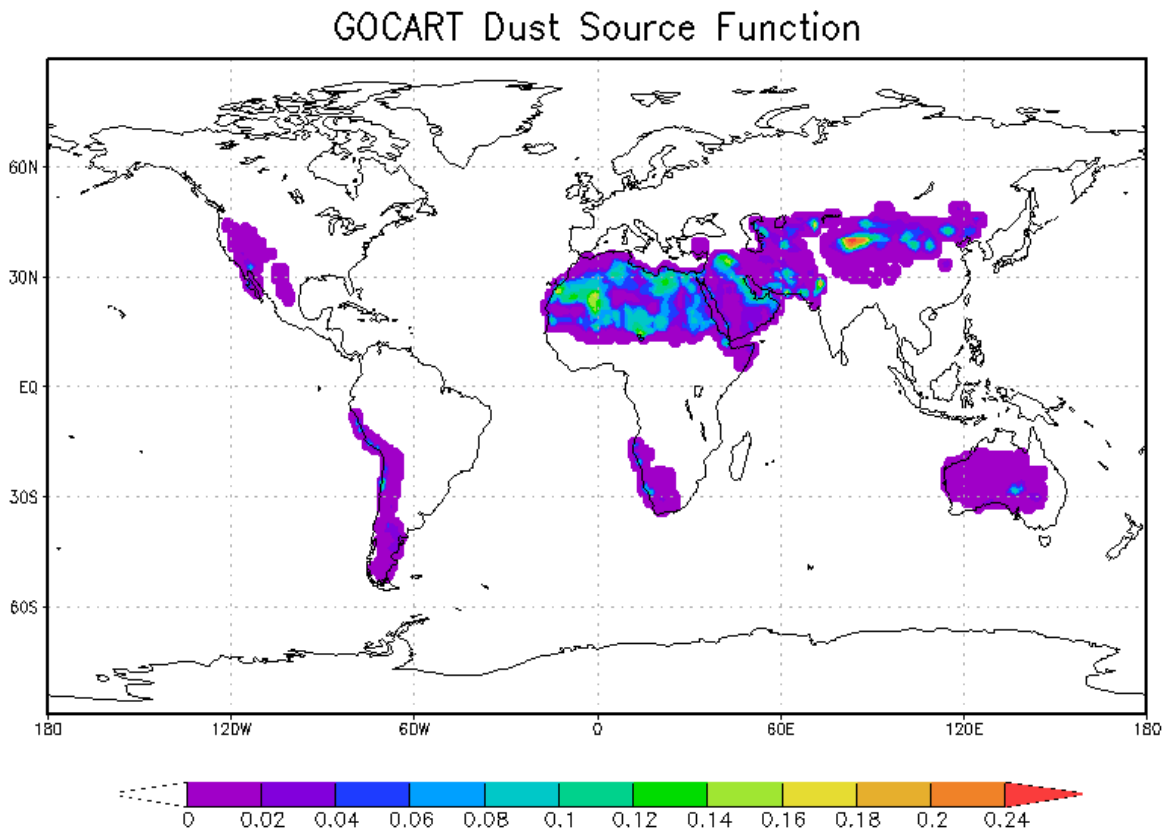
5

6

7



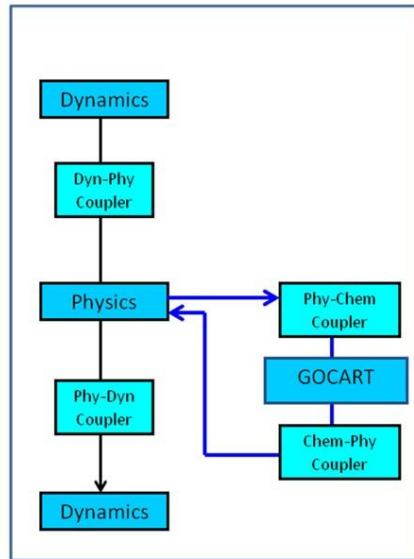
1  
 2 Figure 1. Schematic summary of the GOCART aerosol module as adapted and being  
 3 implemented in GEOS-4/5 at GMAO and NEMS GFS at NCEP.  
 4



1

2 Figure 2. The dust source function or probability of dust uplifting, mapped to GFS T126  
 3 resolution, used in NGAC V1.0.

4

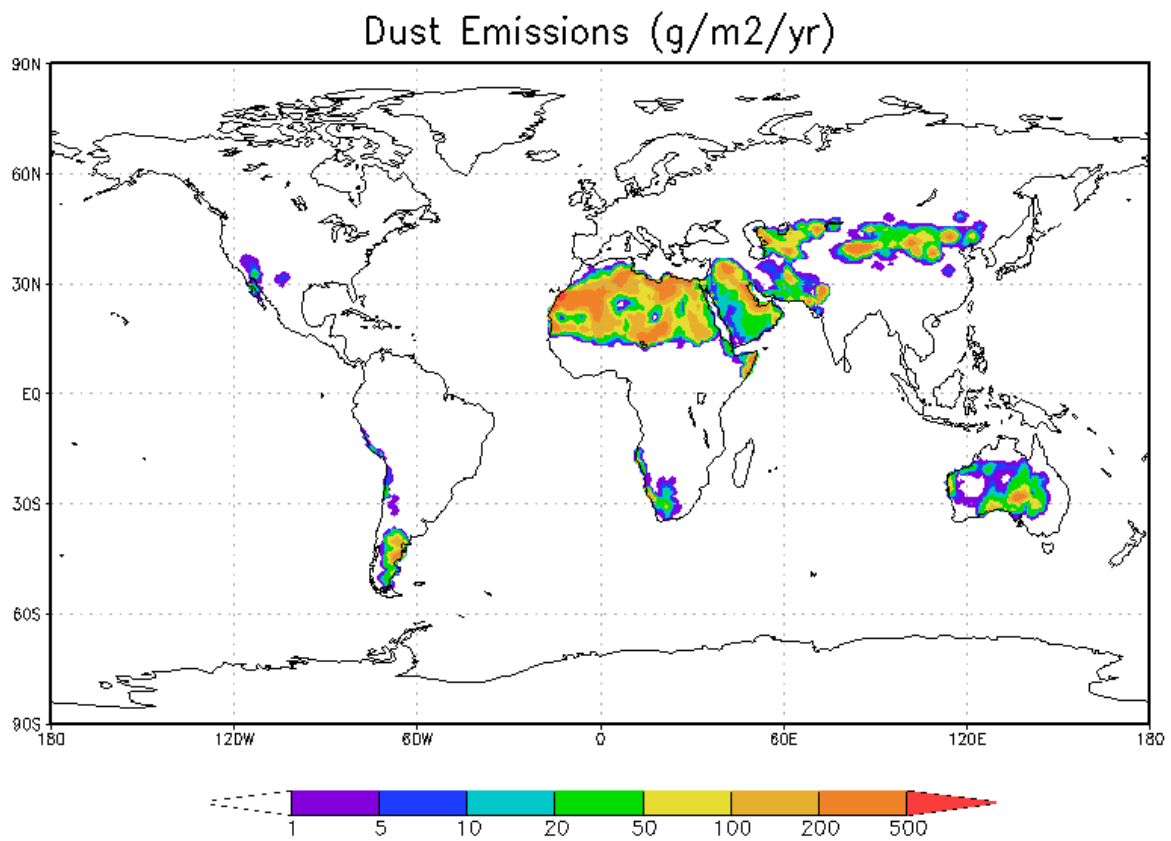


1

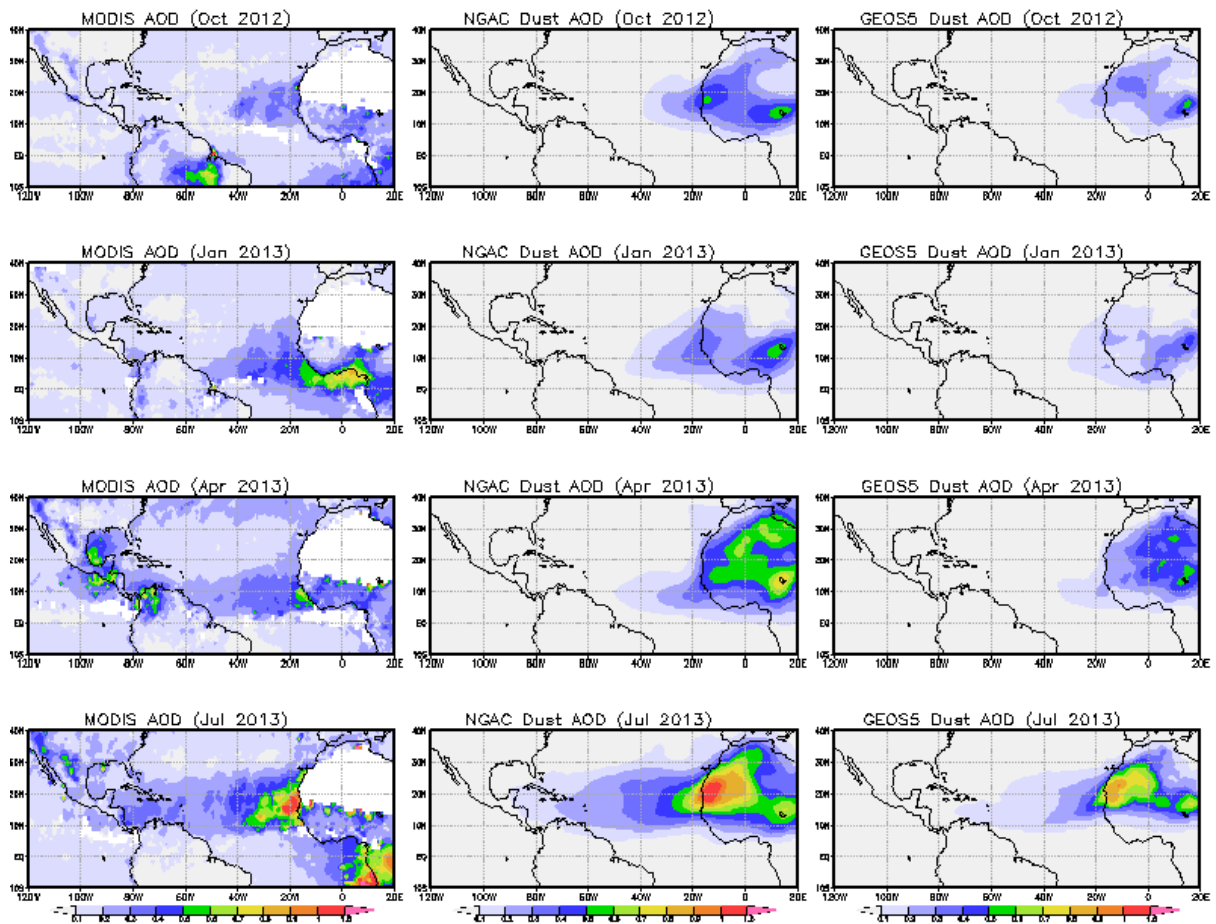
2 Figure 3. Primary integration runstream of NGAC.

3

4



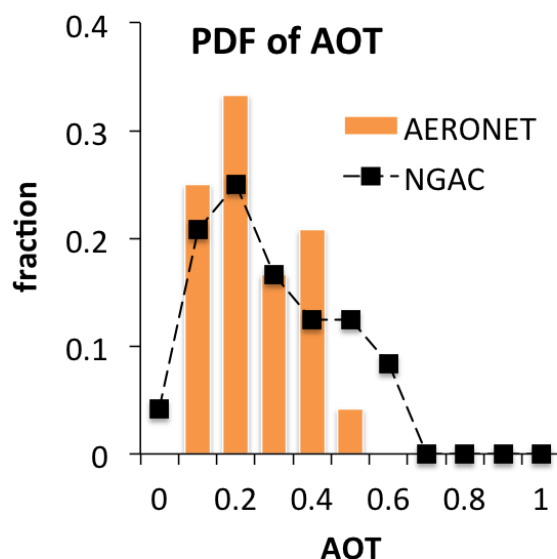
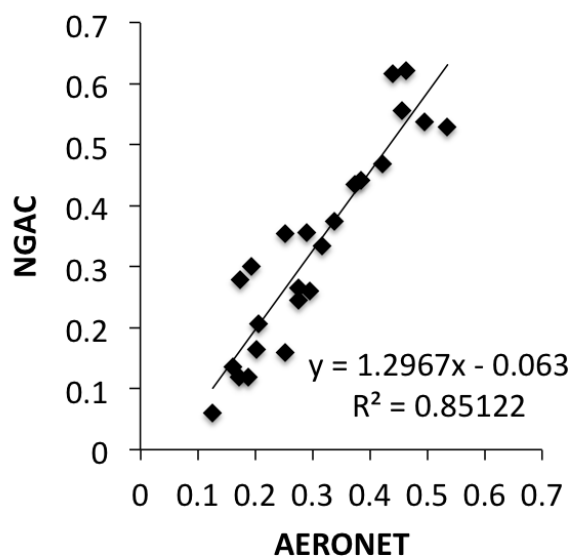
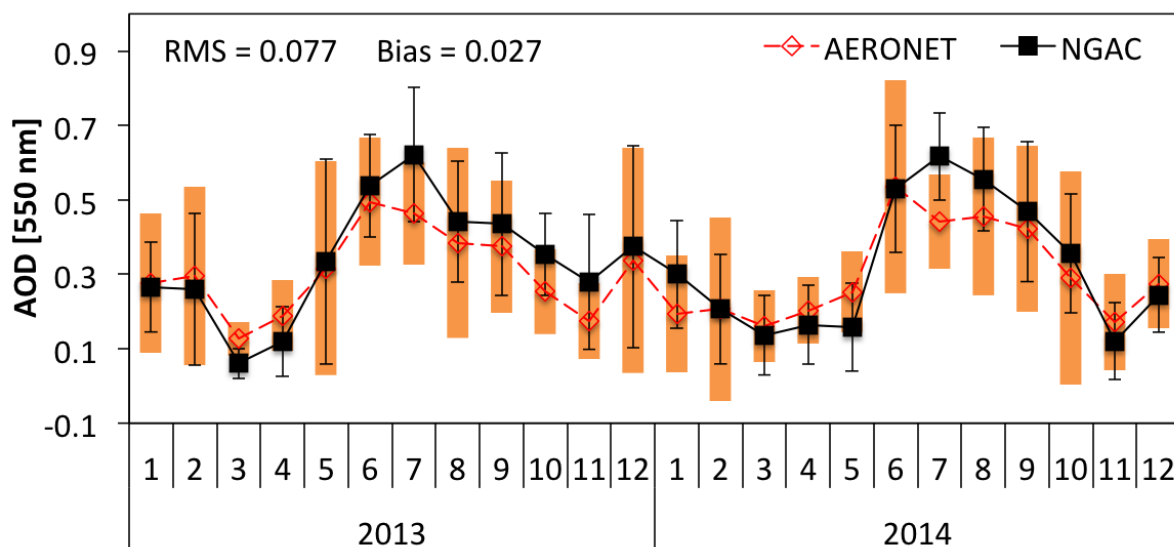
1  
2 Figure 4. Annual dust emissions (in g m<sup>-2</sup> yr<sup>-1</sup>) over the September 2012–September 2013  
3 period.  
4



1  
 2 Figure 5. Comparisons of monthly-mean MODIS total AOD (left), NGAC V1.0 dust AOD  
 3 (middle), and GEOS5 dust AOD (right) at 550 nm for October 2012, January 2013, April  
 4 2013, and July 2013 periods.

5

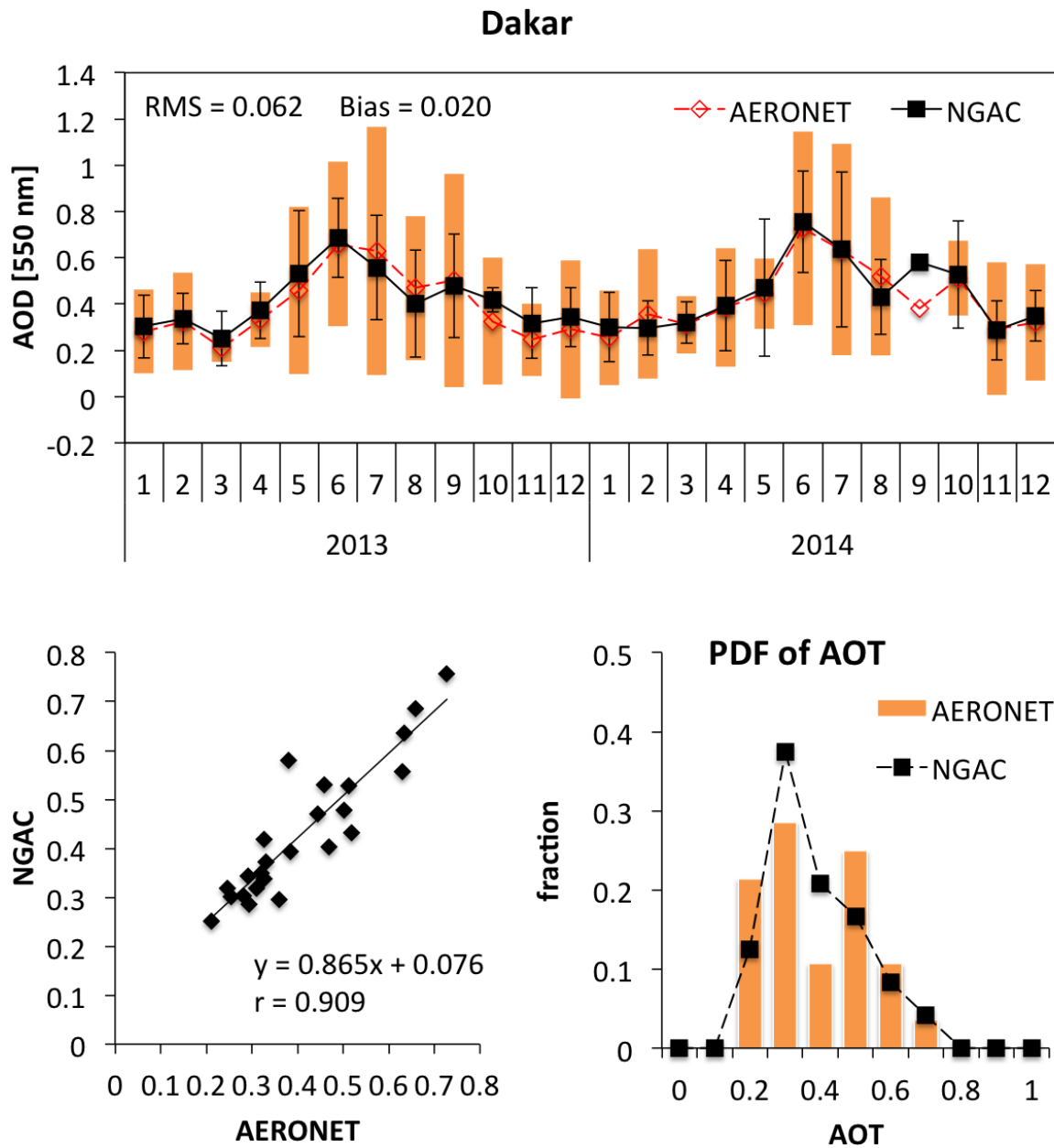
## Cape Verde



1  
2

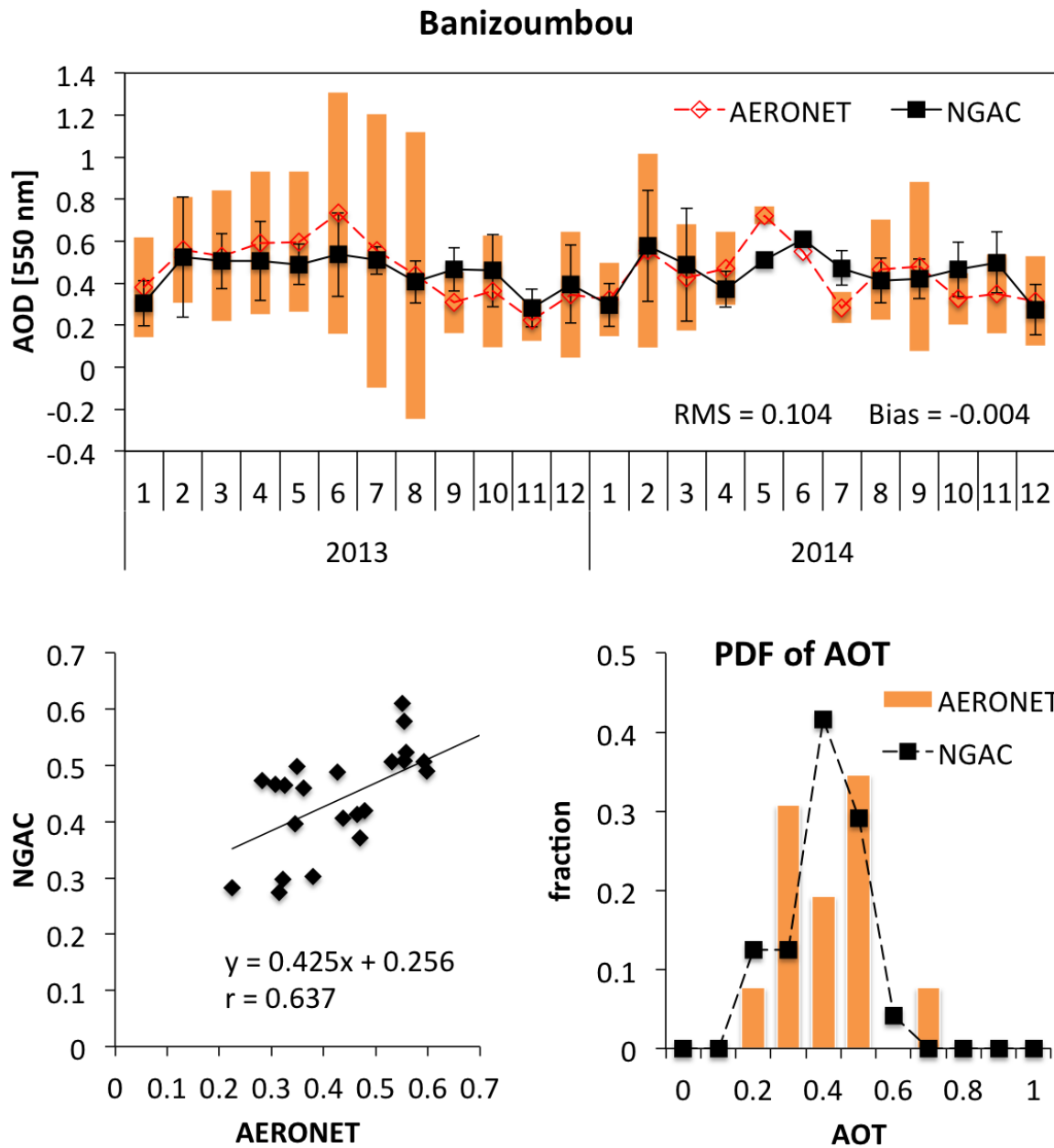
3 Figure 6a. NGAC V1.0 versus L1.5 AERONET 550-nm AOD comparisons at Cape Verde  
4 for the 2013-2014 period: a time series, scatterplot, and fractional distribution histogram. In  
5 the time series, the model monthly means and standard deviation about the mean are shown in  
6 the black symbols and lines. The AERONET monthly means and standard deviation about  
7 the mean are shown in the red shading and orange bars. In the PDF plot, the model is  
8 indicated by the black symbols and line, and the AERONET observations are indicated by  
9 orange bars.





1  
2  
3  
4

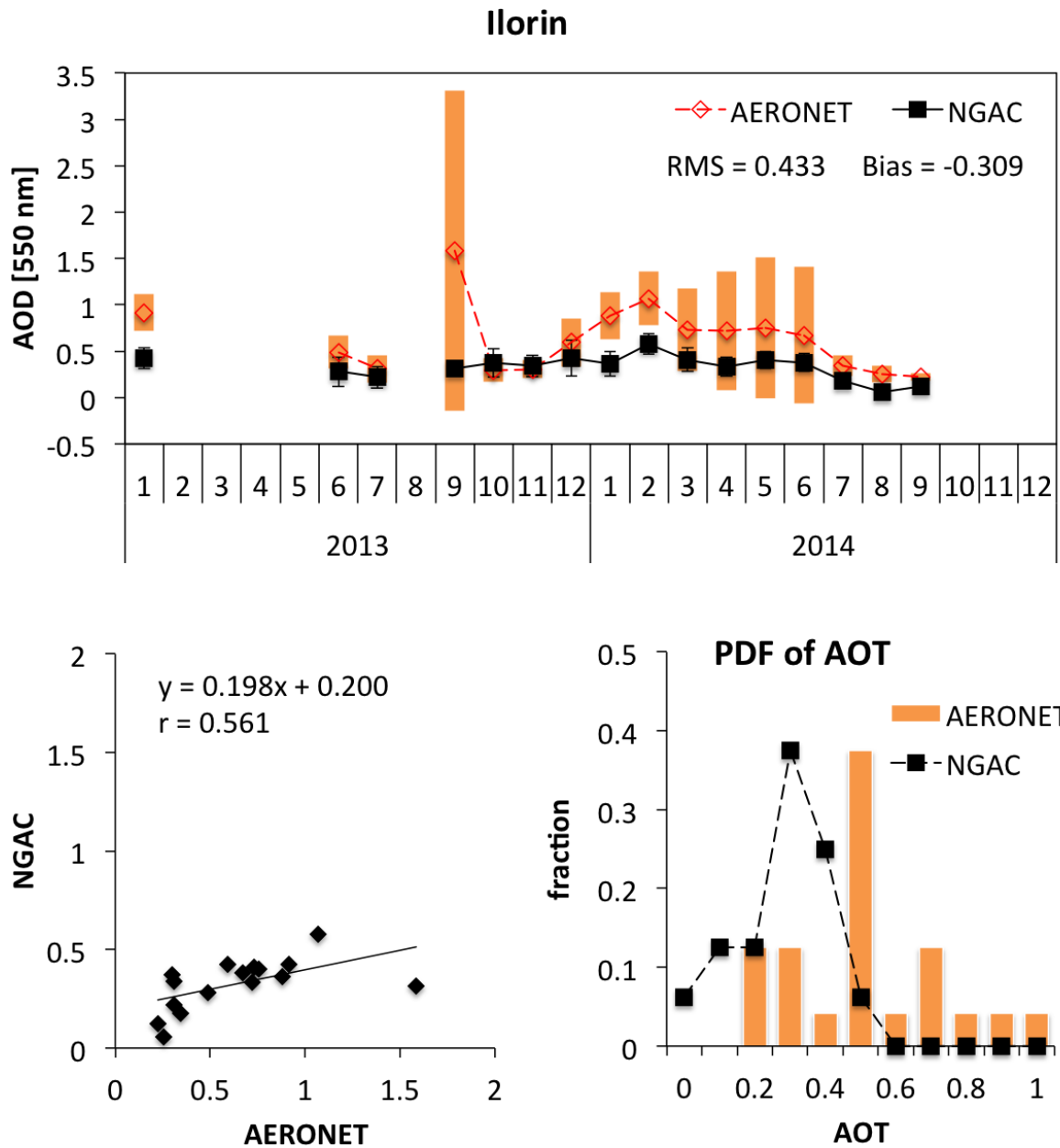
Figure 6b. NGAC V1.0 versus AERONET 550-nm AOD comparisons at Dakar for the 2013-2014 period: a time series, scatterplot, and fractional distribution histogram.



1

2 Figure 6c. NGAC V1.0 vs. AERONET 550 nm AOD comparisons at Banizoumbou for the  
 3 2013 -2014 period: a time series, scatterplot, and fractional distribution histogram.

4

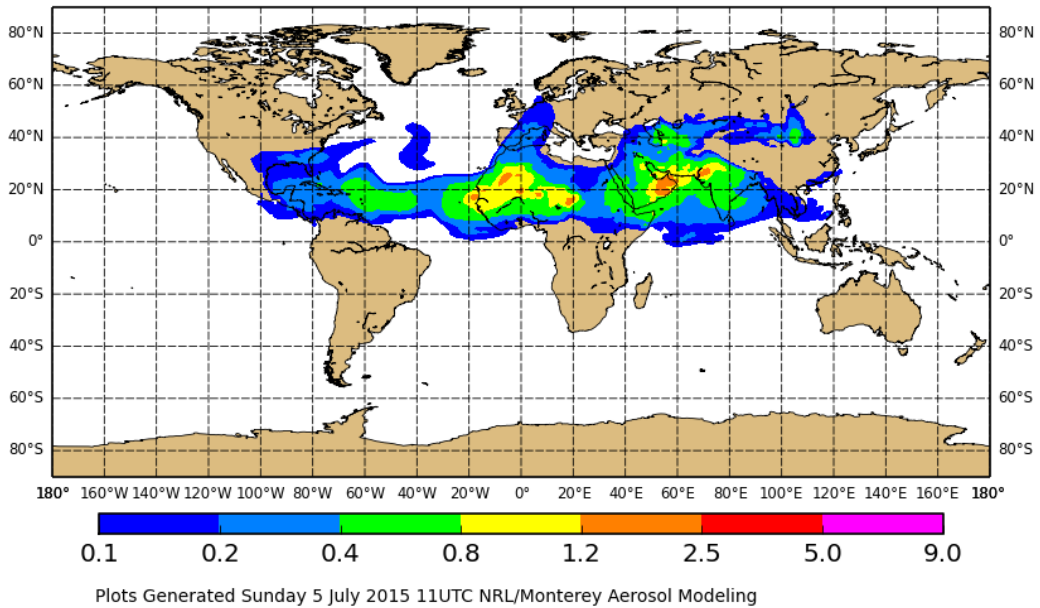


1  
 2 Figure 6d. NGAC V1.0 vs. AERONET 550 nm AOD comparisons Ilorin for the 2013 -2014  
 3 period: a time series, scatterplot, and fractional distribution histogram.  
 4



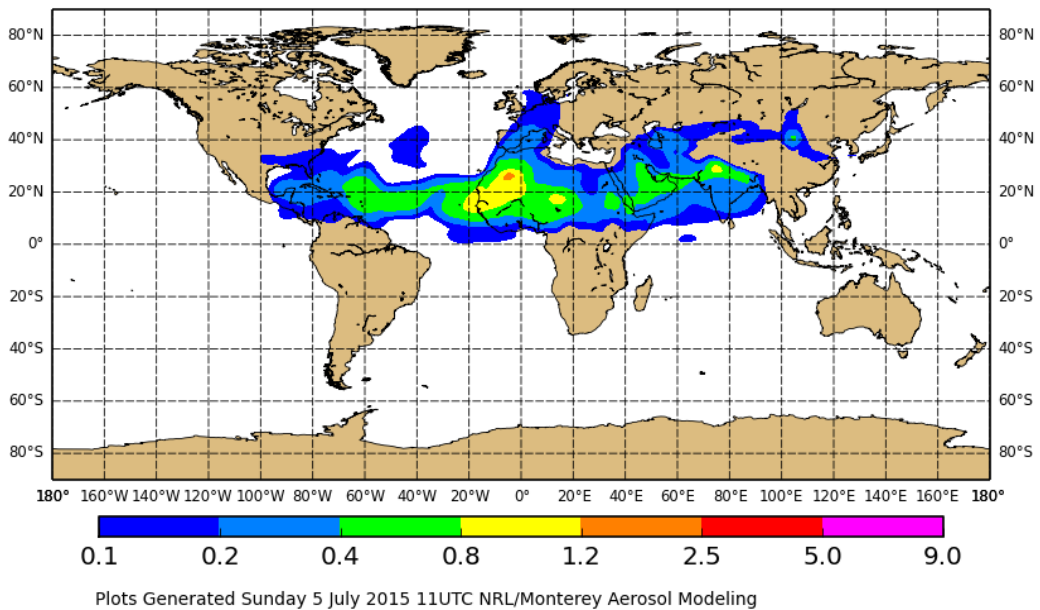


Saturday 4 July 2015 00UTC ICAP Forecast t+012  
 Saturday 4 July 2015 12UTC Valid Time  
 DUST Aerosol Optical Depth at 550nm ( nMEM = 7 )



1

Saturday 4 July 2015 00UTC NGAC Forecast t+012  
 Saturday 4 July 2015 12UTC Valid Time  
 DUST Aerosol Optical Depth at 550nm



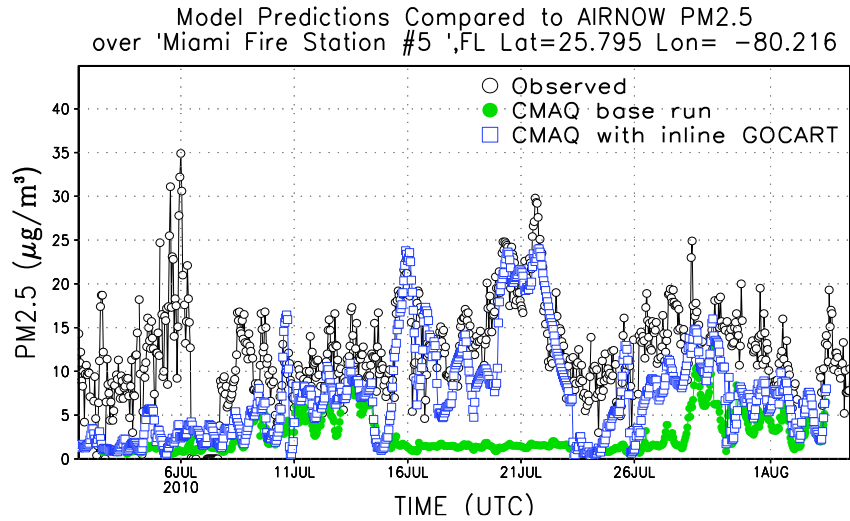
2

3

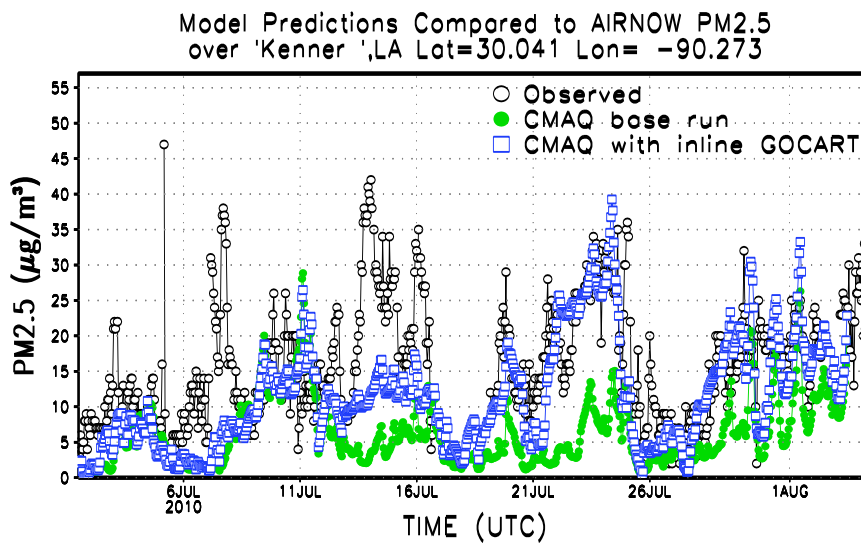
4 Figure 7. Dust AOD valid at 12:00 UTC 4 July 2015 for ICAP multi-model ensemble (top)  
 5 and NGAC V1.0 (bottom). The ensemble is based on 7 members, including the models from  
 6 NCEP (NGAC V1.0), GMAO, ECMWF, NRL, JMA, UKMO, and BSC. These figures are  
 7 produced by the Naval Research Laboratory.

8

1



2



3

4 Figure 8. Time series of PM2.5 from EPA AIRNOW observations (black dot), CMAQ  
5 baseline run using static LBCs (green dot) and CMAQ experimental run using NGAC LBCs  
6 (blue square) at Miami, FL (top panel) and Kenner, LA (bottom panel).

7

8